Intelligent Energy Systems: Introducing Power–ICT Interdependency in Modeling and Control Design

Luca Galbusera, Georgios Theodoridis, and Georgios Giannopoulos

***Abstract*—This paper introduces a novel control scheme for mitigating the cascading effects of a failure in the power transmission grid. Modern power systems include controller entities, which exchange information (measurement/control signals) with the grid through information communication technology (ICT). Nevertheless, networking problems can generate observability/reachability issues, which prevent the controller from correctly estimating the grid's state and applying in a timely manner the necessary actions. Thus, we present a control approach that explicitly takes into account the potential degradation of the ICT performance during power failure events. To this end, the power-induced ICT deficiencies are modeled as additive communication latency, to quantify their impact on the controller's effectiveness. Moreover, in order to overcome excessive/varying delays, a model predictive control architecture is proposed, which produces directives for both the safeguard cut of power lines and the load/generation regulation, in a manner that minimizes the impact of the initial power failure on the overall grid.**

***Index Terms*—Critical infrastructures, interdependencies, model predictive control (MPC), resilience.**

I. Introduction

THE efficiency and resilience of the modern power transmission grids rely on the exploitation of field information, in order for the optimum preventive/mitigating actions to be identified and applied in a timely manner. To this end, real-time measurements of the grid's state are collected and processed, and the computed decisions are provided as control feedback. The communication between the grid and the controller(s) is carried out through an information communication technology (ICT) system that allows for the data exchange [1], [2]. Due to the grave importance of power availability in combination with the inherent ICT vulnerabilities and the complications of the power–ICT integration [3], the study of networked energy grids has attracted significant research effort [4].

Despite its obvious merits, the introduction of networking into energy grids can give rise to rather undesirable phenomena, since 1) the delivery of the power information is subject to the ICT imperfections and 2) the ICT operation itself is dependent on power provision. Therefore, any power failures are expected to be intensified under conditions of degraded ICT performance, which may be caused by either internal (e.g., congestion and equipment failure) or external (e.g., natural disasters and cyber attacks) factors. The coincidence of perturbations affecting both the power and cyber systems is a scenario of particular interest, since some of the most common and disastrous causes of power failures, i.e., intense natural phenomena and orchestrated malicious actions, have a high spatial consistency, affecting colocated power and ICT infrastructure. Under such circumstances, the ICT deficiency inhibits the timely perception of the power anomalies by the controller and the transfer of the response commands back to the grid [5]. Consequently, the power failure keeps spreading due to the cascading overloads, while, at the same time, the initial ICT malfunction is further deteriorated due to the power shortage/damages, causing a continuously accelerating domino effect along both the power and ICT axes.

Hence, it is of primary importance to quantitatively analyze the bidirectional correlation between the power and ICT systems. Furthermore, it is highly beneficial that this modeling facilitates the development of an advanced transmission grid control scheme, capable of effectively incorporating the power–ICT interdependency features into the decision process.

With regard to the interoperability of energy and cyber systems, in addition to the general notions applicable to networked critical infrastructures [6], the emphasis has been primarily laid on the direction of the ICT-to-power impact. In [7], a mechanism is proposed for dealing with network delays and errors in the communication among distributed controllers, and in [8], a scheme is introduced for compensating packet dropouts in both directions of the controller grid communication. Furthermore, special attention has been paid to analyzing and modeling the behavior of the power grid against cyber attacks [9], [10]. The authors in [11] mapped the effect of cyber attacks upon the power grid by means of graph theory, while for the same purpose, the use of simulations on the basis of Bayesian networks is proposed in [12]. Moreover, experimental results on the impact of cyber attacks on the supervisory control and data acquisition functionalities are provided in [13].

On the contrary, the effect of the energy system malfunctions on the ICT operation has either been qualitatively covered [14] or a simplified quantification is usually followed, according to which an ICT node is considered OFF when the collocated electrical node fails [15]. Nevertheless, in addition to neglecting the possible existence of backup power (e.g., uninterruptible power supply (UPS) [16]), such a binary coupling between the power and ICT elements disregards the underlying complexity

Manuscript received February 28, 2014; revised March 4, 2014, June 6, 2014, and July 25, 2014; accepted September 14, 2014. Date of publication October 22, 2014; date of current version March 6, 2015.

The authors are with the Institute for the Protection and Security of the Citizen, European Commission Joint Research Centre, 21027 Ispra, Italy (e-mail: luca.galbusera@jrc.ec.europa.eu; georgios.theodoridis@jrc.ec.europa.eu; georgios.giannopoulos@jrc.ec.europa.eu).

Digital Object Identifier 10.1109/TIE.2014.2364546

of the network that actually realizes the data connectivity. Thus, considering that delay is the primary impact of ICT operation on reliable monitoring/control applications, we hereby propose a delay-based nondiscrete modeling of the effects of power malfunctions on ICT information transmission. This way, delay is introduced as the common ground for a realistic analysis framework of networked transmission grids, including bidirectional correlations.

Furthermore, it is essential to develop an advanced power control scheme that is aware of the power–ICT interdependencies. To this end, our approach is extended in the direction of electrical grid resilience optimization methods [17]. In view of our delay-based representation of interdependency, we particularly focus on delay compensation schemes, many of which have been proposed in the framework of power systems [18], [19]. One of the most prominent techniques to deal with such problems is model predictive control (MPC), which has been extensively applied so far to electrical management problems [20]–[22]. More specifically, some recent contributions have included distributed/decentralized architectures [23], [24] and networked control applications [25], while computational considerations have been also taken into account [26]–[28].

The basic notion is to exploit the delay-compensation features of MPC in order to play against the same variable we use to model interdependency, i.e., the communication delay, and to provide grid reconfiguration in a timely manner. Our controller reacts to both the nonidealities that can affect the information transmission (including interdependency-induced delays) and the structure of the observed network topology, which dynamically varies depending on the ICT performance. From this point of view, the receding horizon feature of MPC helps to keep track of the changes affecting the system progressively, following the critical event. In our formulation, the central controller can both induce the preventive tripping off of some lines and modulate generation and load of the accessible grid nodes in order to counteract possible cascading effects affecting the transmission lines.

The rest of this paper is organized as follows. In Section II, we introduce our representation of the power and ICT subsystems. Section III provides the modeling of the impact of power failures upon the operation of any collocated ICT infrastructure, and in Section IV, the delay-aware control architecture is described. Finally, Section V presents numerical experiments, and in Section VI, the conclusions are drawn. For ease of reference, a nonexhaustive list of the used symbols is provided in Table I.

TABLE I
LIST OF SYMBOLS AND NOTATIONS USED

$\mathcal{S}=\{\mathcal{N},\mathcal{E}\}$	Power grid graph, consisting of nodes $\mathcal{N}$ and edges $\mathcal{E}$
$(\cdot)^I$	ICT elements
$(\cdot)^V$	Viable (perceived by the controller) grid elements
M, W	Grid's arc-node incidence, and reactance matrix
G, L, P	Power nodes' generation, load, and power
F, x	Power lines' power, and effective power
ψ, ϕ	Power lines' on/off state (failure or tripping off)
$(\cdot)_n$ and $(\cdot)_e$	Specific node and line of reference
$\hat{(\cdot)}$	Estimated/predicted quantities
$(\cdot)_{(j)}$, $(\cdot)_{[j]}$	Actual and control island of reference
$\hat{B}_{[j]}$	Estimated border power of the j^{th} control island
δ_n^{add}	Nodes' communication delay overhead due to power problems
δ_n^{gc}, δ_n^{cg} (δ_e^{gc}, δ_e^{cg})	Nodes' (power lines') communication delay to/from the controller
$(\cdot)'$	Transpose of a matrix
$\lvert\cdot\rvert$	Cardinality of a set
$\bar{\cdot}$	One and the same arbitrary row is removed

II. SMART TRANSMISSION GRID DESCRIPTION AND FORMULATION

Modern electrical transmission systems consist of three interoperable subsystems, i.e., the power grid, the controller, and the ICT network providing connectivity between the two. Here, we describe the main attributes of the power transmission grid and the ICT.

A. Energy Subsystem

The electrical subsystem is represented as a directed graph, consisting of a constant set of nodes interconnected through a time-varying set of edges, i.e., $\mathcal{S}(\tau)=\{\mathcal{N},\mathcal{E}(\tau)\}$, $\tau\in\mathbb{N}_0$. Time $\tau=0$ corresponds to the nominal operating state of the electrical grid, when no infrastructural or operational alterations have occurred yet. The power grid at its nominal state $(\mathcal{S}(0))$ is a *connected* graph, i.e., a single power island.

Given the broad penetration of distributed energy resources, each electrical node at transmission level is in general the aggregation of both generation and load. Hence, for the set of nodes $(\mathcal{N})$, the instantaneous generation $G(\tau)$ and load $L(\tau)$ vectors are defined, with $G(\tau),L(\tau)\in\mathbb{R}_+^{|\mathcal{N}|}$ and $G(\tau)\in[G^{\min},G^{\max}]$ and $L(\tau)\in[L^{\min},L^{\max}]$. Assuming that a total generation and load shedding is possible per node, $G^{\min}=L^{\min}=0$. Although $\mathcal{N}$ is static, $G(\tau)$ and $L(\tau)$ are functions of time. These variations of $G(\tau)$ and $L(\tau)$ do not result from alterations in the generation capabilities or the load demands, since such changes are negligible in the short time scale of a grid failure event. On the contrary, they are caused by the regulation of generation and load, which are, in turn, carried out in order to cope with power unbalances and line overloads after infrastructural failures. Therefore, unless power line failures occur, $G(\tau)=G(0)$ and $L(\tau)=L(0)$, i.e., both power production and load remain equal to their nominal values. The power balance condition for $\mathcal{S}(0)$ is expressed as

$$\sum_{n\in\mathcal{N}}G_n(0)=\sum_{n\in\mathcal{N}}L_n(0). \tag{1}$$

It should be noted that, in spite of the continuous decentralization of power generation, the points of major power generation and consumption are in general not colocated. Thus, the energy grid nodes $(n\in\mathcal{N})$ are usually characterized either by $G_n(0)/L_n(0)\gg 1$ (regions of major energy consumption, e.g., residence and industrial areas) or by $G_n(0)/L_n(0)\ll 1$ (regions of major energy production, e.g., power plants, connection points of power importing lines).

The set $\mathcal{E}(\tau)\subseteq\mathcal{E}(0)$ represents the transmission lines of the grid still operating at time τ. Every edge ends at two different nodes, and any pair of nodes is only connected with a single edge. Moreover, each edge is oriented, to define the power flow direction. The initial set of edges $(\mathcal{E}(0))$ is the

overall set of available transmission lines. Any alterations to this set are the result of lines' failures. No establishment of new transmission lines or recovery of previously failing ones is considered. Thus, $\mathcal{E}(\tau_2) \subseteq \mathcal{E}(\tau_1)$, $\forall \tau_2 > \tau_1 \in \mathbb{N}_0$. The topology of the electrical grid $(\mathcal{S}(\tau))$ at each time instance is fully described by a directional arc-node incidence matrix $M(\tau)$ of size $|\mathcal{N}| \times |\mathcal{E}(0)|$. Furthermore, the reactance matrix W is defined, which is a $|\mathcal{E}(0)| \times |\mathcal{E}(0)|$ diagonal matrix, whose elements of the main diagonal are equal to the reactance of the respective transmission line. Then, according to the dc power model [29], the vector of the power flows $(F(\tau))$, $\forall \tau \in \mathbb{N}_0$ as long as a single island topology exists, is [30]

$$F(\tau) = W^{-1}\bar{M}(\tau)' \left(\bar{M}(\tau)W^{-1}\bar{M}'(\tau)\right)^{-1} \bar{P}(\tau) \qquad (2)$$

where $P(\tau) = G(\tau) - L(\tau)$ is the vector of the nodes' algebraic power, and $\bar{\cdot}$ indicates that one and the same arbitrary row is removed from all matrices, for the system of equations to have a single solution under condition (1).

Although $\mathcal{S}(0)$ is a single-island electrical grid, any line failure (due to either preventive tripping off or damage by accident/overload) may result in its splitting into multiple islands, whose number, composition, and connectivity vary in time. Hence, any island j composed at time τ is associated to the graph $\mathcal{S}_{(j)}(\tau) = \{\mathcal{N}_{(j)}, \mathcal{E}_{(j)}(\tau)\}$, where $\mathcal{N}_{(j)} \subseteq \mathcal{N}$, and $\mathcal{E}_{(j)}(\tau) \subseteq \mathcal{E}(\tau)$, with $|\mathcal{N}_{(j)}| \geq 1$ and $|\mathcal{E}_{(j)}(\tau)| \geq 0$. Thus, (1) and (2) are, in general, applied per island, i.e.,

$$\sum_{n\in\mathcal{N}_{(j)}} G_n(\tau) = \sum_{n\in\mathcal{N}_{(j)}} L_n(\tau) \qquad (3)$$

$$F_{(j)}(\tau) = W_{(j)}^{-1}\bar{M}'_{(j)}(\tau) \times \left(\bar{M}_{(j)}(\tau)W_{(j)}^{-1}\bar{M}'_{(j)}(\tau)\right)^{-1} \bar{P}_{(j)}(\tau). \qquad (4)$$

Remark 1: A power equilibrium is feasible for island j, if

$$\sum_{n\in\mathcal{N}_{(j)}} G_n^{\max} \geq \sum_{n\in\mathcal{N}_{(j)}} L_n^{\min}, \sum_{n\in\mathcal{N}_{(j)}} G_n^{\min} \leq \sum_{n\in\mathcal{N}_{(j)}} L_n^{\max}. \qquad (5)$$

Every transmission line $e \in \mathcal{E}(0)$ is characterized by a maximum sustainable power (capacity) $C_e > 0$ determined by the specifications of its elements, i.e., the ending transformers and the cabling. Any increase in the flowing power above this limitation is bound to cause the failure of the line, due to damage or local preventive tripping off, which can be the root cause of the cascading phenomena.

Nevertheless, because of the overall inertia of the electrical system, any changes in the nodes' state (generation/load levels) or connectivity (line failures) are not imminently experienced by the remaining infrastructure. Additionally, the lag in a line's failure when its capacity is exceeded is primarily the result of the necessary time for the tripping-off mechanisms to be triggered or the structural materials (cables, transformers) to collapse due to the consequent noxious drift in thermal equilibrium. Therefore, according to [31], in order to model the inertia of the transmission grid infrastructure against changes in the operating conditions, we introduce the *effective power flow* $(x(\tau))$ for all the still operating lines $(\mathcal{E}(\tau))$. We will describe the evolution of this quantity from the initial condition $x(0) = F(0)$ according to the following discrete-time model:

$$x(\tau+1) = (1-\alpha)x(\tau) + \alpha F(\tau) \qquad (6)$$

where $\alpha \in [0, 1]$ is a fixed constant mainly dependent upon the size of the discretization step.

In this respect, let $\psi_e(\tau)$ be the binary event that line e fails at time τ, where $e \in \mathcal{E}(\tau - 1)$, i.e., the line e is one of the lines still operating at time $\tau - 1$. Then,

$$\psi_e(\tau) = \begin{cases} 1, & \text{if } |x_e(\tau)| > C_e \\ 0, & \text{otherwise.} \end{cases}$$

However, in addition to the failure due to damage or local tripping off, a line can be also cut following a central control directive. The key difference between the automated switching off of a line at local level and its disconnection due to a control command is that the former case regards an instinctive response of the local protection switch that has the unique goal of preventing the line's destruction without taking into consideration the possible impact on the rest of the grid. Therefore, a transfer of the failure to neighboring lines because of cascading overloads is likely. On the contrary, in the latter case, the line cutting action is the result of a consolidated control decision aimed at the overall grid's stability and efficient operation. Thus, in addition to $\psi_e(\tau)$, the binary quantity $\phi_e(\tau)$ is introduced, which will be equal to 1 if a control signal enforcing the disconnection of line e is received at time τ, at any of the two ending nodes of line e.

Eventually, the set of electrical edges at any time τ is defined on the basis of the following rule:

$$OR(\psi_e(\tau_1), \phi_e(\tau_1)) = 1 \Leftrightarrow e \notin \mathcal{E}(\tau_2) \qquad \forall \tau_2 \geq \tau_1.$$

B. ICT Subsystem

The ICT subsystem is represented as an undirected connected graph $\mathcal{S}^I = \{\mathcal{N}^I, \mathcal{E}^I\}$ constant in time. Each ICT node, which corresponds to networking equipment (e.g., a formation of routers), is considered to be directly matched to an electrical node (assuming collocation), so that each element $n \in \mathcal{N}$ is coupled with $n \in \mathcal{N}^I$. Moreover, the controller is considered as an additional networking element (node) with index equal to 0 by convention. Thus, $|\mathcal{N}^I| = |\mathcal{N}| + 1$. On the contrary, no coupling is assumed between $\mathcal{E}^I$ and $\mathcal{E}$. The one-to-one matching between the electrical and ICT nodes is fully justified in the case of the transmission grid, due to the high aggregation applied to our transmission-level representation and analysis. Each node corresponds to a broad geographical area, grouping together all the area's respective elements (power or ICT).

The overall architecture of the combined energy–ICT–controller scheme is depicted in Fig. 1. The monitoring data consist of the power flow $(F(\tau))$ and the "failing due to overload" attribute $(\psi(\tau))$ for the set of power transmission lines $(\mathcal{E}(\tau))$, while the controller directives cover the generation and load $(G(\tau), L(\tau))$ for the set of power nodes $(\mathcal{N})$ and the "cut by the controller" signal $(\phi(\tau))$ for $(\mathcal{E}(\tau))$. The line-related information is sent from/to both the attached nodes.

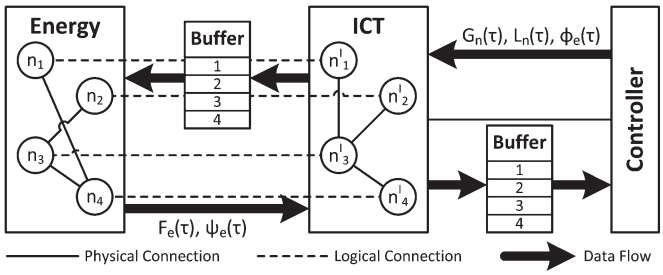

Fig. 1. Block diagram of the smart transmission grid.

Moreover, a regular time-stamping process is applied to follow the sequence of the monitoring and control information. To this end, the monitoring and control elements (the energy grid agents and the central controller) are normally equipped with an input *buffer*, which provides the necessary functionality for storing the received data and selecting the most updated information available.

III. Modeling of Power-to-ICT Impact

This section provides a quantitative approximation of the possible impact of power failures upon the cyber subsystem of the transmission grid. Before proceeding with the mere analysis of the power-to-ICT correlation, it is essential to underline that the ultimate goal of this study is to enhance the efficiency of the response to anomalies in the power delivery process, by appropriately consolidating the control decisions to overcome cyber imperfections. Therefore, the devised model does not need to scrutinize the alterations in the ICT state as a function of the dynamic power behavior, but it only needs to macroscopically identify at which extent this additional ICT perturbation affects back the power system itself, in particular, concerning the power failure cascading.

In general, the efficiency of a communication system that supports monitoring and control operations is evaluated in terms of its ability to provide the error-free delivery of the transmitted data within the time boundaries that are imposed by the serviced application. In order to provide the error-free data exchange, the transport layer of these ICT systems is implemented on the basis of reliable protocols, such as the predominant Transmission Control Protocol [8], which effectively retransmit the data packets until their correct reception. Hence, the error-free data exchange can be eventually taken for granted, regardless of the exact architectural (e.g., Internet or proprietary links) and technological characteristics of the traversed networks (e.g., physical medium, modulation, and error detection/correction) and their dynamically varying performance (e.g., channel losses, congestion, and equipment failures).

On the contrary, due to the reliable nature of the transport layer, the network performance eventually has a grave impact on the communication delay, since the unsuccessful data deliveries are continuously reattempted. Thus, any ICT infrastructural/operational malfunctions causing data packet errors or dropouts ultimately increase the connections' latency. However, this time distortion of the exchanged data can result in the suboptimal or even failing operation of the energy grid, since the control decisions and the applied actions will be based on obsolete, out-of-synchronization (data with regard to the state of different power nodes at the same time instance arrive at different times), or missing information. Therefore, regardless of the exact root cause and the internal consequences of the ICT problems, their perceivable effect on the dependent power system can be assessed in terms of delay levels (infinite delay stands for complete lack of communication because of nonexisting network path).

The ICT infrastructure of a smart transmission grid can be classified into two categories: 1) the *last-mile* segment, which is colocated with the energy grid elements that perform the measurements and apply the control actions, and 2) the *backbone*, which is responsible for the long-distance transfer of data. In general, the ICT equipment is prioritized as critical load, and thus, it is usually protected in case of load shedding (selective blackouts). Moreover, the last-mile equipment and the backbone nodes of higher hierarchy are supported by backup power resources, such as UPSs or generators. Therefore, the uninterruptible operation of the major ICT nodes of the smart grid for a medium-term time horizon is achieved.

Nevertheless, the unconditional resilience of the backbone against power disruptions, particularly for the nodes of lower hierarchy, cannot be taken for granted either if a dedicated network or a public Internet Service Provider is used. Furthermore, unless direct UPS support exists, the ICT shall still fail in the short term, since there is an idle time for the backup solutions (generators, emergency power lines) to come into duty, plus the necessary time for the network devices to boot and reestablish connections after the disruption. This lag in ICT restoration exactly after the power failure is critical for the mitigation of the cascading effects. Additionally, apart from the power-to-ICT impact due to lack of power supply, ICT perturbation can be also caused by the damage of the ICT equipment, either from the same event (e.g., accident and physical phenomena) that triggered the initial power failure or from its consequences, since power overloads are often followed by physical destruction (e.g., fire) of the corresponding facilities (e.g., high-voltage transformers and substations).

Consequently, it becomes apparent that 1) the data delivery performance can be highly affected by anomalies in the electrical grid and 2) a strict quantification of this correlation for the general case is not feasible, since a vast range of spatiotemporally dynamic or even unpredictable factors is involved. In this respect and based on the delay effect of the ICT imperfections, the impact of power failures upon the ICT performance is most suitable to be indicated by means of an additive delay imposed by the respective ICT nodes. Hence, considering the decrease in the amount of serviced load as the measure of the power perturbation, the additive delay $\delta_n(\tau)$ experienced by any data traversing the ICT node $n \in \mathcal{N}^I \setminus \{0\}$ at time τ is formulated by the following relationship:

$$\delta_n(\tau) = \begin{cases} 0, & \text{if } L_n(\tau) \geq L_n^{\text{th}} \\ \delta_n^{\text{add}}, & \text{otherwise} \end{cases} \tag{7}$$

where $L_n(\tau)$ is the serviced load at the matching electric node (see Section II-B), and L_n^{th} is the load threshold above which no impact on the ICT operation is considered. Furthermore, δ_n^{add} is

a parameter predefined for each ICT node, to quantify the level of ICT perturbation due to power problems.

In this representation, δ_n^{add} quantifies the power-to-ICT effect, whereas L_n^{th} describes the sensitivity in the coupling of the corresponding power and ICT nodes. This definition of $\delta_n(\tau)$ in (7) facilitates the nonbinary (no ON-to-ON or OFF-to-OFF dependency) mapping of power imperfections to ICT behavior in such a way that the resulting ICT perturbation is derived in terms of the quality of service (QoS) perceived by the power system itself. Thus, the study of the cascading impact of a power failure on each subsystem separately and on the overall transmission grid is enabled. Furthermore, this modeling approach particularly fits the low-resolution representation of the transmission grid, where each electrical (ICT) node corresponds to an aggregation of multiple interconnected electrical (ICT) elements, and thus, the detailed topologies and attributes of the two systems at the points of their interdependencies are hidden. Moreover, the presence of additive delay at the ICT nodes also caters for the need to analyze the systems' interdependency under conditions of ICT perturbation due to external reasons, e.g., cyber attacks.

Finally, by summing up the additive delay per ICT node with the delay of the traversed ICT links throughout the communication path, the total delay imposed on the data exchange procedure can be calculated. The aggregate delay for the data received by the controller from node n (grid-to-controller delay) at time τ is $\delta_n^{\text{gc}}(\tau)$, and the aggregate delay for the data received by node n from the controller (controller-to-grid delay) at time τ is $\delta_n^{\text{cg}}(\tau)$. In general, $\delta_n^{\text{gc}}(\tau) \neq \delta_n^{\text{cg}}(\tau)$, due to the possible changes in the ICT state during the information forwarding. Correspondingly, for each line e, we define $\delta_e^{\text{gc}}(\tau) = \min\{\delta_{n_1}^{\text{gc}}(\tau), \delta_{n_2}^{\text{gc}}(\tau)\}$ and $\delta_e^{\text{cg}}(\tau) = \min\{\delta_{n_1}^{\text{cg}}(\tau), \delta_{n_2}^{\text{cg}}(\tau)\}$, where n_1 and n_2 are the ends of edge e. For future discussion, we will assume $\delta_n^{\text{gc}}(\tau), \delta_n^{\text{cg}}(\tau), \delta_e^{\text{gc}}(\tau), \delta_e^{\text{gc}}(\tau) \in \mathbb{N}$, for all τ, e, and n.

IV. Interdependency-Aware Control Design

This section proposes a control architecture based on MPC. This control technique exploits the prediction of the system's response to control inputs in order to optimize a finite-time performance index subject to constraints [32], [33]. According to the receding horizon principle, new samples of the process under control becoming available from time to time are exploited by performing the optimization cyclically. Each time, the controller will produce a stream of control signals referred to a rolling time horizon. Only the initial portion of these controls will be applied, until more updated control signals become available. This predictive feature is often exploited in situations like the one considered in this paper, i.e., time gaps due to communication delays have to be taken into account.

In addition, in our setup, the ICT may induce important differences in the delays affecting the information flow from each source to its destination. Our approach consists in identifying an excessive delay in the information reception as an indicator of malfunction. In this respect, we will draw a delay-based distinction between the viable and unviable parts of the electrical grid. The control formulation will be defined for the viable portion of it, taking into account estimated power flows involving the unviable parts of the grid, as well.

A. Viable Graph

The objective of the electrical grid topology estimation is to define the controller's inner estimate of the ICT-accessible portion of the electrical grid. In the presence of limited assumptions on the ICT network performance, this can be done by means of a delay-based criterion, consisting in the definition of the viable node set $\mathcal{N}^V(\tau) = \{n \in \mathcal{N} : \delta_n^{\text{gc}}(\tau) \leq \delta_{\text{th}}^{\text{gc}}\}$, where $\delta_{\text{th}}^{\text{gc}} \in \mathbb{N}$ is a fixed threshold. According to this definition, if no recent enough information has been received from a given electrical node, this is considered inaccessible also as a receiver of control signals. Similarly, we can also define the set of viable electrical lines $\mathcal{E}^V(\tau) = \{e \in \mathcal{E}(0) : \delta_e^{\text{gc}}(\tau) \leq \delta_{\text{th}}^{\text{gc}}\}$. Consequently, bottlenecks due to different ICT nodes along the communication path defined by the adopted transmission protocol also contribute to the viability discrimination, qualified by graph $\mathcal{S}^V(\tau) = \{\mathcal{N}^V(\tau), \mathcal{E}^V(\tau)\}$.

B. State Prediction

Predicting the electrical grid's time evolution is complicated by the nonuniform delay affecting the information arriving at the controller from the different nodes. This discrepancy will be covered by defining $b_\tau = \tau - \min\{\delta_e^{\text{gc}}(\tau),\ \forall e \in \mathcal{E}^V(\tau)\}$ and constructing the state estimate $\hat{x}_e(b_\tau)$ based on the state information available about each edge, i.e., $x_e(\tau - \delta_e^{\text{gc}}(\tau)),\ \forall e \in \mathcal{E}^V(\tau)$. Instant b_τ will be considered as a baseline time for prediction and control. Denote by $\hat{x}_e(k|\tau)$ the state prediction for edge e computed at time τ and referred to time k and by h_τ the prediction horizon defined at time τ, which we will choose so that $h_\tau > \tau - b_\tau$ so that the prediction is not obsolete by default when produced.

Now, consider a graph $\hat{\mathcal{S}}(\tau) = \{\hat{\mathcal{N}}(\tau), \hat{\mathcal{E}}(\tau)\}$, whose construction will be specified later and such that $\hat{\mathcal{N}}(\tau) \equiv \mathcal{N}^V(\tau), \hat{\mathcal{E}}(\tau) \subseteq \mathcal{E}^V(\tau)$. Based on (6), for each control island j in $\hat{\mathcal{S}}(\tau)$, we introduce the following state predictor, $\forall k \in [b_\tau, b_\tau + h_\tau - 1]$:

$$\hat{x}_{[j]}(k+1|\tau) = (1-\alpha)\hat{x}_{[j]}(k|\tau) + \alpha \hat{F}_{[j]}(k|\tau) \tag{8}$$

where

$$\hat{x}_{[j]}(b_\tau|\tau) = \hat{x}_{[j]}(b_\tau) \tag{9}$$

$$\hat{F}_{[j]}(k|\tau) = \bar{R}_{[j]}(\tau)\bar{\hat{P}}_{[j]}(k|\tau) \tag{10}$$

$$\bar{R}_{[j]}(\tau) = W_{[j]}^{-1}\bar{\hat{M}}'_{[j]}(\tau)\left[\bar{\hat{M}}_{[j]}(\tau)W_{[j]}^{-1}\bar{\hat{M}}_{[j]}(\tau)'\right]^{-1} \tag{11}$$

$$\bar{\hat{P}}_{[j]}(k|\tau) = \bar{\hat{G}}_{[j]}(k|\tau) - \bar{\hat{L}}_{[j]}(k|\tau) + \bar{\hat{B}}_{[j]}(k|\tau). \tag{12}$$

Equation (9) is the predictor initialization; at the start, it will correspond to the nominal operation values of the electrical grid. The power flow (4) is replicated in the controller's viability-based framework by (10); the terms on the right side therein are specified in (11) and (12). In (11), $\hat{M}(\tau)$ is the arc-node incidence matrix associated to $\hat{\mathcal{S}}(\tau)$, whereas W is

assumed to be known to the controller. Notably, the predicted power load/generation balance $\hat{P}_{[j]}(k|\tau)$ inside the jth control island results from predicted generation $\hat{G}_{[j]}(k|\tau)$ and load $\hat{L}_{[j]}(k|\tau)$ to be assigned by our controller, in combination with the estimated border power flow $\hat{B}_{[j]}(k|\tau)$. This quantity, by convention, will be considered as positive if entering the node, and it will be taken into account in the control synthesis procedure. Different estimation methods can be applied for it, e.g., taking a constant value or considering the (delayed) expected effect of previous control decisions on the plant's performances.

Formulas (8)–(12) rely on the assumption that the topology of the jth control island stays unmodified along the considered prediction horizon. For consistency, this implies that the predicted states should not exceed the capacity values leading to failures, e.g., $|\hat{x}_{[j]}(k|\tau)| \leq C_{[j]},\ \forall\, k \in [b_\tau+1, b_\tau+h_\tau]$. To meet this requirement, we will define $\hat{\mathcal{S}}(\tau)$ by introducing specific constraints in our MPC formulation and performing a feasibility check taking $\mathcal{S}^V(\tau)$ as a starting point, which possibly leads to edge removals. As for $\hat{x}_{[j]}(b_\tau)$, the fulfillment of the capacity constraint is ensured by the fact that $\hat{\mathcal{E}}(\tau) \subseteq \mathcal{E}^V(\tau)$.

C. MPC Controller

In the control design, we consider as control variables the generation and load levels of the nodes qualified as viable, as well as the possible controlled cutting of some lines among those connected to them. The idea consists of two key elements: 1) associating the possible line cutting to the solution of a feasibility test attached to the proposed predictive control formulation, leading to the definition of $\hat{\mathcal{S}}(\tau)$ at each instant τ, and 2) predicting optimal generation and load sequences to be sent to the grid nodes. At the electrical grid level, the most feasible predictions will be actuated taking into account the delay affecting the transit of the control signals via the ICT.

Now, assume that $\hat{\mathcal{S}}(\tau)$ has been specified, and let $\hat{\mathbf{G}}_{[j]}(\tau) = [\hat{G}_{[j]}(b_\tau|\tau)', \ldots, \hat{G}_{[j]}(b_\tau + h_\tau - 1|\tau)']'$ and $\hat{\mathbf{L}}_{[j]}(\tau) = [\hat{L}_{[j]}(b_\tau|\tau)', \ldots, \hat{L}_{[j]}(b_\tau + h_\tau - 1|\tau)']'$ denote generation and load values inside each control island $\hat{\mathcal{S}}_{[j]}(\tau)$. According to the receding horizon control principle, our MPC controller will solve, at each instant $\tau \geq 0$ and for each control island, the following constrained finite-time optimal control problem:

$$\min_{\hat{\mathbf{G}}_{[j]}(\tau), \hat{\mathbf{L}}_{[j]}(\tau)} J\left(\hat{x}_{[j]}(b_\tau), \hat{\mathbf{G}}_{[j]}(\tau), \hat{\mathbf{L}}_{[j]}(\tau)\right) \tag{13}$$

$$\text{s.t.} \quad \forall\, k \in [b_\tau, b_\tau + h_\tau - 1]$$

$$(8) - (12) \tag{14}$$

$$|\hat{x}_e(k+1|\tau)| \leq C_e \qquad \forall\, e \in \hat{\mathcal{E}}_{[j]}(\tau) \tag{15}$$

$$\hat{G}_{[j]}(k|\tau) \in \left[G^{\min}_{[j]}, G^{\max}_{[j]}\right] \tag{16}$$

$$\hat{L}_{[j]}(k|\tau) \in \left[L^{\min}_{[j]}, L^{\max}_{[j]}\right] \tag{17}$$

$$\sum_{n \in \hat{\mathcal{N}}_{[j]}(\tau)} \left[\hat{G}_n(k|\tau) - \hat{L}_n(k|\tau) + \hat{B}_n(k|\tau)\right] = 0 \tag{18}$$

where, fixing a weighting coefficient $\beta \geq 0$,

$$J\left(\hat{x}_{[j]}(b_\tau), \hat{\mathbf{G}}_{[j]}(\tau), \hat{\mathbf{L}}_{[j]}(\tau)\right) = \sum_{k=b_\tau}^{b_\tau+h_\tau-1} \left[\mu_1\left(\hat{L}_{[j]}(k|\tau) - L_{[j]}(0)\right) + \beta\mu_2\left(\hat{x}_{[j]}(k+1|\tau)\right)\right] \tag{19}$$

and μ_1, μ_2 are suitable convex functions. Formula (19) is meant to put together two priorities typically found in electrical transmission grid management problems: supporting the load request and limiting the grid risks due to line overloads. The constraint set also obeys the same principles: (14) is the previously introduced state predictor, and (15) prescribes the fulfillment of the capacity constraints specific to each line; (16) and (17) are bounds to the generation and load for each node within control island j; (18) represents the power balance condition, comprehensive of the estimated border power flows. As the MPC problem is solved at each instant, the controller will track the system's changes progressively according to the most updated data coming from the plant.

At each instant, the computation of the optimal solution to the problem discussed above will be preceded by a constraint feasibility check leading to the specification of $\hat{\mathcal{S}}(\tau)$. Define $\hat{B}^{\max}_n(\tau) = \max_{k \in [b_\tau, b_\tau+h_\tau-1]} \hat{B}_n(k|\tau)$ and $\hat{B}^{\min}_n(\tau) = \min_{k \in [b_\tau, b_\tau+h_\tau-1]} \hat{B}_n(k|\tau)$, for each $n \in \hat{\mathcal{N}}(\tau)$. Then, the following theorem is related to the feasibility of the MPC problem formulated above.

Theorem 1: Assume

$$\sum_{n \in \hat{N}_{[j]}(\tau)} \left[G^{\max}_n - L^{\min}_n + \hat{B}^{\min}_n(\tau)\right] \geq 0 \tag{20}$$

$$\sum_{n \in \hat{N}_{[j]}(\tau)} \left[G^{\min}_n - L^{\max}_n + \hat{B}^{\max}_n(\tau)\right] \leq 0. \tag{21}$$

Assume also that, for all $\tilde{G}_n \in \{G^{\min}_n, G^{\max}_n\}$, $\tilde{L}_n \in \{L^{\min}_n, L^{\max}_n\}$, and $\tilde{B}_n(\tau) \in \{\hat{B}^{\min}_n(\tau), \hat{B}^{\max}_n(\tau)\}$, $\forall\, n \in \hat{N}_{[j]}(\tau)$

$$\left|\bar{R}_{[j]}(\tau)\left(\bar{\tilde{G}}_{[j]} - \bar{\tilde{L}}_{[j]} + \bar{\tilde{B}}_{[j]}(\tau)\right)\right| \leq C_{[j]}. \tag{22}$$

Then, problem (13)–(18) formulated at time τ is feasible for the jth control island.

Proof: First, observe that conditions (20) and (21) imply the feasibility of (18), in view of (16) and (17) and the definition of $\hat{B}^{\max}_n(\tau)$ and $\hat{B}^{\min}_n(\tau)$. By definition, $\hat{\mathcal{S}}(\tau)$ is such that $\hat{\mathcal{E}}(\tau) \subseteq \mathcal{E}^V(\tau)$; thus, it only contains edges $e \in \mathcal{E}(\tau - \delta^{\text{gc}}_e(\tau))$, which fulfill $|x_e(\tau - \delta^{\text{gc}}_e(\tau))| \leq C_e$. As a consequence, since by (9) we have $|\hat{x}_e(b_\tau|\tau)| \leq C_e$, if $|\hat{F}_e(b_\tau|\tau)| \leq C_e$ in view of (8), it will follow that also $|\hat{x}_e(b_\tau+1|\tau)| \leq C_e$, $\forall e \in \hat{\mathcal{E}}(\tau)$. Extending the same condition to the entire prediction horizon, condition $|\hat{F}_e(k|\tau)| \leq C_e,\ \forall e \in \hat{\mathcal{E}}_{[j]}(\tau)$, and $\forall k \in [b_\tau, b_\tau + h_\tau - 1]$, ensures the feasibility of constraint (15). Finally, according to (10)–(12), we can rewrite the latter condition for the jth control island as

$$\left|\bar{R}_{[j]}(\tau)\left(\bar{\hat{G}}_{[j]}(k|\tau) - \bar{\hat{L}}_{[j]}(k|\tau) + \bar{\hat{B}}_{[j]}(k|\tau)\right)\right| \leq C_{[j]}.$$

Then, replacing $\hat{G}_{[j]}(k|\tau)$, $\hat{L}_{[j]}(k|\tau)$, and $\hat{B}_{[j]}(k|\tau)$ with $\tilde{G}_{[j]}$, $\tilde{L}_{[j]}$, and $\tilde{B}_{[j]}(\tau)$, the feasibility of (15) is translated into a boundary check represented by condition (22).

A special point of interest about the latter result is that it provides a tool for defining line cuts preventing critical situations, as far as both service provision and infrastructure preservation are concerned. An option in this sense is to initialize $\hat{\mathcal{S}}(\tau)$ as $\mathcal{S}^V(\tau)$ at each step. Then, assigning line cutting costs to both internal and border lines of each island j found in it, we will calculate the minimal-cost line removal that ensures feasibility, leading to an updated definition of $\hat{\mathcal{S}}(\tau)$. Now, we define $\hat{\phi}^V(\tau)$ as the selected line cut referred to the viable set $\mathcal{E}^V(\tau)$ leading to feasibility; this may also include no cuts. These controller-induced line cuts that are defined and computed at time τ will produce effects on the variable ϕ_e through the mediation of the ICT network. The following corollary, whose proof is trivial, is a simple consequence of Theorem 1.

Corollary 1: Assuming $L^{\min} = G^{\min} = 0$, a cut $\hat{\phi}^V(\tau)$ ensuring the feasibility of the control problem (13) exists at each time instant τ.

In order to complete this subsection, we propose Algorithm 1 for the definition of the control actions in our interdependency-aware design, where $\tau_{\max}$ denotes the simulation time, and $j^V_{\max}(\tau)$ denotes the number of islands in $\mathcal{S}^V(\tau)$.

Algorithm 1 Interdependency-aware control algorithm

initialization: $\mathcal{S}(0)$, W, $P(0)$, C, $F(0)$, and $x(0)$;
for $\tau = 0 : \tau_{\max}$ **do**
  get updates from the plant;
  define b_τ, estimate $\hat{x}_e(b_\tau)$, $\forall e \in \mathcal{E}^V(\tau)$, fix h_τ;
  estimate $\mathcal{S}^V(\tau)$ and initialize $\hat{\mathcal{S}}(\tau) \equiv \mathcal{S}^V(\tau)$;
  for $j = 1 : j^V_{\max}(\tau)$ **do**
    perform the feasibility check and define $\hat{\phi}^V(\tau)$;
    update $\hat{\mathcal{S}}(\tau)$;
  end for
  define $j_{\max}(\tau)$ as the number of islands in $\hat{\mathcal{S}}(\tau)$;
  for $j = 1 : j_{\max}(\tau)$ **do**
    solve the MPC problem (13)–(18) for $\hat{\mathbf{G}}_{[j]}(\tau)$, $\hat{\mathbf{L}}_{[j]}(\tau)$;
  end for
  transmit the controls (line trip off, generation, load) to the viable lines and nodes;
end for

D. Control Signals Transmission and Distortion Compensation

As we have already discussed, the effectiveness of the control action can critically depend on the viability properties and, consequently, on the accessibility of the electrical nodes. ICT delays, data packet disorder, and modifications to the communication paths significantly affect the quality of the transmission process. This also implies that the reconfiguration control signals from the controller to the plant can be partially received and with variable delays according to the situation, resulting in a distortion over the original controller's messages. Moreover, the operational conditions of the grid itself may have changed at the same time.

A first consequence of these considerations is that the controlled cuts $\phi(\tau)$ applied at time τ may not match the complete set of selected line cuts defined by the controller. Furthermore, in general, a compensation is required inside the electrical nodes in order to cope with the balancing requirement (3). To this end, conditions (5) are assumed to be fulfilled in the hereafter analysis. The discrepancy compensation is generally supposed to involve all nodes in a given island j existing in the grid at time τ, irrespective of their instantaneous accessibility by the controller. Let $G_{(j),a}(\tau)$ and $L_{(j),a}(\tau)$ denote the values of generation and load assigned to each node in the considered island. In order to overcome the ICT delays, $G_{(j),a}(\tau)$ and $L_{(j),a}(\tau)$ are chosen by first considering the most updated arrays of control predictions received by each electrical node from the plant and, second, by selecting among the array's prediction values the most suitable one based on a minimal time discrepancy principle.

Now, the objective is to assign the actual balanced values for $G_{(j)}(\tau)$ and $L_{(j)}(\tau)$, for each electrical island j existing at time τ. This is done trivially if $\sum_{n\in\mathcal{N}_{(j)}(\tau)}[G_{n,a}(\tau) - L_{n,a}(\tau)] = 0$, i.e., the island is power balanced. Otherwise, a matching of the offered generation with the requested load is performed, on the basis of the local power balance compensation mechanisms that inherently exist in large traditional power generation facilities (e.g., increasing the angle velocity of generators and shedding local loads). Specifically, if in island j the generation assigned by the controller exceeds the connected load $(\sum_{n\in\mathcal{N}_{(j)}(\tau)}[G_{n,a}(\tau) - L_{n,a}(\tau)] > 0)$, then,

- if $\sum_{n\in\mathcal{N}_{(j)}(\tau)}[G^{\min}_n - L_{n,a}(\tau)] \le 0$, the generation at all the island's nodes is proportionally decreased until $\sum_{n\in\mathcal{N}_{(j)}(\tau)}[G_n(\tau) - L_n(\tau)] = 0$, subject to $G_{(j)}(\tau) \in [G^{\min}_{(j)}, G^{\max}_{(j)}]$;
- if $\sum_{n\in\mathcal{N}_{(j)}(\tau)}[G^{\min}_n - L_{n,a}(\tau)] > 0$, the load at all the island's nodes is proportionally increased (if possible, as, for example, where water dams or other energy storage mechanisms exist), while keeping $G_{(j)}(\tau) = G^{\min}_{(j)}$, until $\sum_{n\in\mathcal{N}_{(j)}(\tau)}[G_n(\tau) - L_n(\tau)] = 0$, subject to $L_{(j)}(\tau) \in [L^{\min}_{(j)}, L^{\max}_{(j)}]$.

On the contrary, the reverse procedure is followed when $\sum_{n\in\mathcal{N}_{(j)}(\tau)}[G_{n,a}(\tau) - L_{n,a}(\tau)] < 0$:

- if $\sum_{n\in\mathcal{N}_{(j)}(\tau)}[G^{\max}_n - L_{n,a}(\tau)] \ge 0$, power is balanced by increasing generation up to the aggregate requested load;
- if $\sum_{n\in\mathcal{N}_{(j)}(\tau)}[G^{\max}_n - L_{n,a}(\tau)] < 0$, the generation is maximized $(G_{(j)}(\tau) = G^{\max}_{(j)})$, and a proportional load shedding is applied.

V. Numerical Experiments

Here, we consider an application of the proposed control architecture to an electrical grid composed of 14 nodes and 20 lines. The topology is taken from the IEEE 14-bus test system, represented in Fig. 2, and the reactance values are chosen according to the prototype. We assume that each bus contains

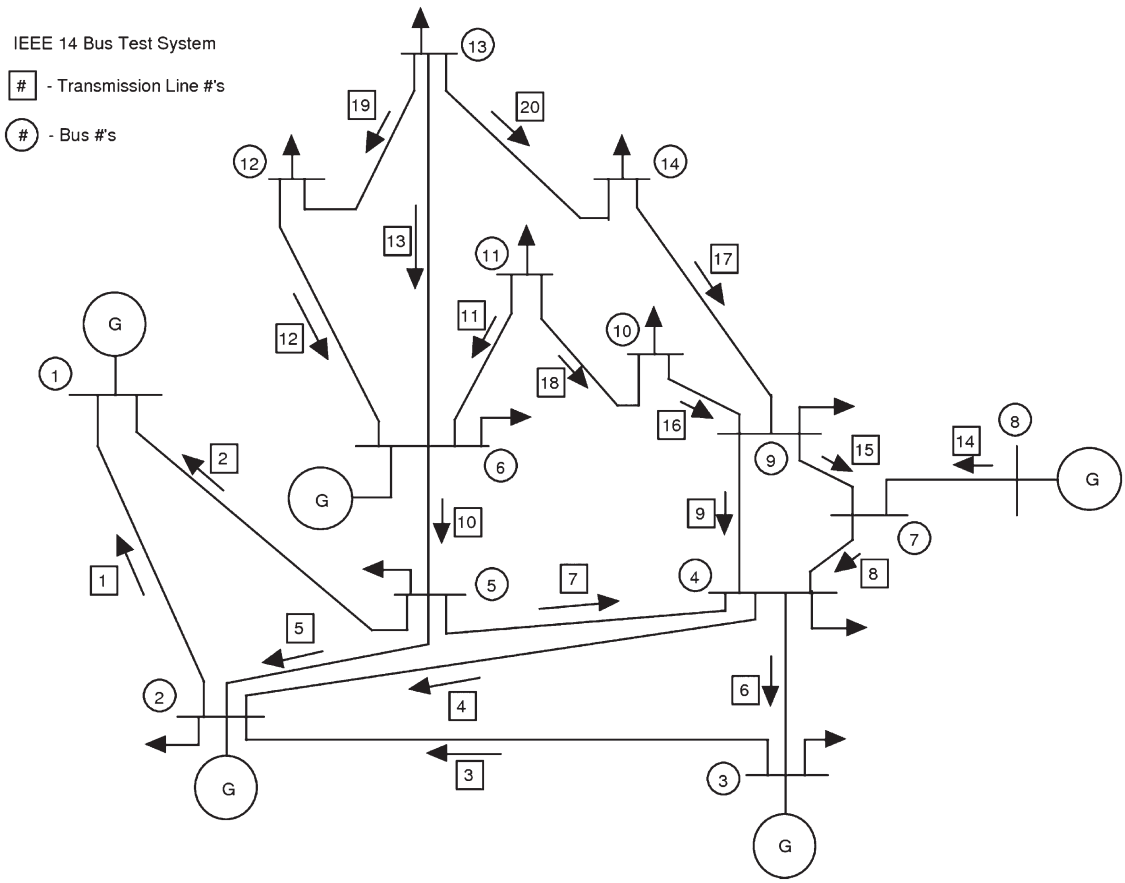

Fig. 2. IEEE 14-bus test system.

both load and generation. In particular, bus 1 provides over 30% of the total power generation in the grid, while its load amounts to about 0.02%. The considered scenario consists in the failure of line 1, leading to a reduced connectivity between node 1 and the rest of the grid. Moreover, the ICT topology matches the one of the electrical grid, with the controller connected to ICT nodes 4, 5, 6, and 11. We study the effects of the value of the interdependency delay constant δ_n^{add} entering (7) (the same for all nodes, i.e., $\delta_n^{\text{add}} = \delta^{\text{add}}$, $\forall\, n \in \mathcal{N}^I \setminus \{0\}$). It must be highlighted that the exact choice of the ICT topology is not critical for the particular purposes of our analysis, since the efficiency of the MPC algorithm is primarily affected by the encountered delays between the controller and the distributed controlled nodes. Hence, in order to acquire a generic evaluation of the system's operation, it is important to consider a wide range of ICT QoS levels regardless of the specific interconnection of the ICT nodes. To this end, different values of delay are taken into account (δ^{add}), for the performance of the proposed control scheme to be widely tested.

In formula (19), we fix, $\forall\, \tau$ and $\forall\, k \in [b_\tau, b_\tau + h_\tau - 1]$,

$$\mu_1\left(\hat{L}_{[j]}(k|\tau) - L_{[j]}(0)\right) = \sum_{n\in\hat{\mathcal{N}}(\tau)} \left(\hat{L}_n(k|\tau) - L_n(0)\right)^2$$

$$\mu_2\left(\hat{x}_{[j]}(k+1|\tau)\right) = \sum_{e\in\hat{\mathcal{E}}_{[j]}(\tau)} \left(\max(0, q_e \hat{x}_e^2(k+1|\tau) - 1)\right)$$

where q_e is chosen to penalize the predicted states when they get close to or exceed the line capacity, $\forall\, e \in \hat{\mathcal{E}}_{[j]}(\tau)$. As an output of our simulations, in Fig. 3, we report the number of lines tripped off by the controller along with the total number of lines off eventually being nonoperational, both expressed as functions of the interdependency delay constant. It can be observed that the controller contributes to the preservation of the lines from damages due to cascading overload by means of preventing line tripping off. Furthermore, in Fig. 4, we represent the reduction to the supported load with respect to the grid's

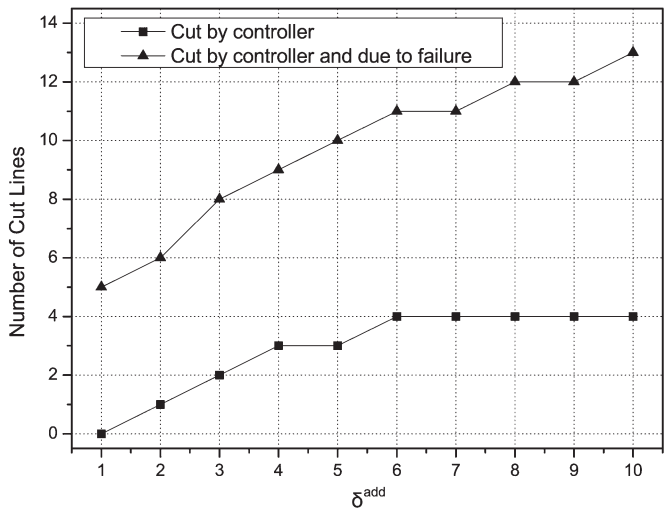

Fig. 3. Number of lines ultimately cut by the controller and the total lines off as a function of the interdependency delay.

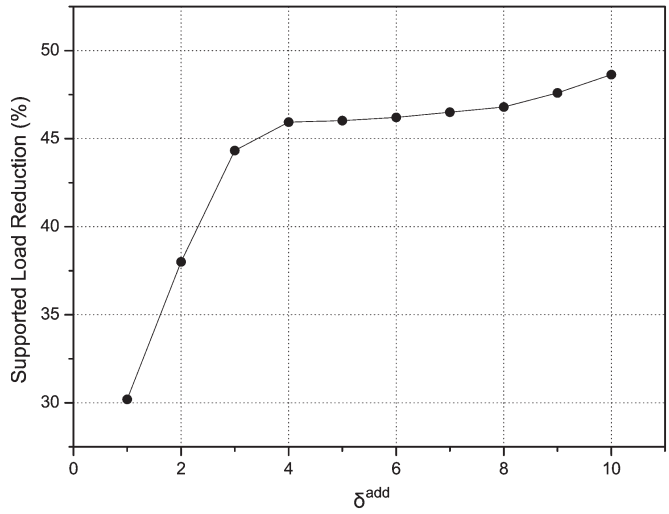

Fig. 4. Reduction in the supported load with respect to the grid's nominal conditions.

nominal conditions, which consistently increments against the increase interdependency-related delay.

VI. Conclusion

This paper has presented an interdependency-aware approach for modeling and controlling an ICT-enabled power transmission grid. The basic principle was to model the effect of power shortage on the performances of the ICT network in terms of delay. In the same framework, we formulated an MPC-based control algorithm to tackle the problem of cascading effects induced by the failure of some electrical lines. One of the novelties of our approach was that we explicitly considered the role of the interdependency-induced delay and grid accessibility in order to provide a timely action on the grid, which was based on a combination of controlled line cutting and load/generation rebalancing actions. Further research on the topic will deal with distributed control architectures and with an evaluation of the impact of specific network features (e.g., controller centrality and network clustering) on the effectiveness of the proposed solutions. In addition, further studies will be devoted to analytic interdependency modeling approaches and to the effects of specific classes of threats primarily affecting the information infrastructure, e.g., ineffective communication protocols and cyber attacks.

References

[1] B. Krogh and P. Kokotovic, "Feedback control of overloaded networks," *IEEE Trans. Autom. Control*, vol. AC-29, no. 8, pp. 704–711, Aug. 1984.
[2] B. Chaudhuri, R. Majumder, and B. C. Pal, "Wide-area measurement-based stabilizing control of power system considering signal transmission delay," *IEEE Trans. Power Syst.*, vol. 19, no. 4, pp. 1971–1979, Nov. 2004.
[3] W. Kröger and E. Zio, "Properties of critical infrastructures," in *Vulnerable Systems*. London, U.K.: Springer-Verlag, 2011, pp. 9–31.
[4] X. Fang, S. Misra, G. Xue, and D. Yang, "Smart grid—The new and improved power grid: A survey," *IEEE Commun. Surveys Tuts.*, vol. 14, no. 4, pp. 944–980, 2012.
[5] A. Bobbio *et al.*, "Unavailability of critical SCADA communication links interconnecting a power grid and a Telco network," *Reliab. Eng. Syst. Saf.*, vol. 95, no. 12, pp. 1345–1357, Dec. 2010.
[6] S. Rinaldi, J. Peerenboom, and T. Kelly, "Identifying, understanding, analyzing critical infrastructure interdependencies," *IEEE Control Syst.*, vol. 21, no. 6, pp. 11–25, Dec. 2001.
[7] Q. Shafiee *et al.*, "Robust networked control scheme for distributed secondary control of islanded microgrids," *IEEE Trans. Ind. Electron.*, vol. 61, no. 10, pp. 5363–5374, Oct. 2014.
[8] H. Li and Y. Shi, "Network-based predictive control for constrained nonlinear systems with two-channel packet dropouts," *IEEE Trans. Ind. Electron.*, vol. 61, no. 3, pp. 1574–1582, Mar. 2014.
[9] P. Mohajerin Esfahani, M. Vrakopoulou, K. Margellos, J. Lygeros, and G. Andersson, "Cyber attack in a two-area power system: Impact identification using reachability," in *Proc. ACC*, Jun. 2010, pp. 962–967.
[10] S. Sridhar, A. Hahn, and M. Govindarasu, "Cyber-physical system security for the electric power grid," *Proc. IEEE*, vol. 100, no. 1, pp. 210–224, Jan. 2012.
[11] D. Kundur, X. Feng, S. Liu, T. Zourntos, and K. Butler-Purry, "Towards a framework for cyber attack impact analysis of the electric smart grid," in *Proc. IEEE Int. Conf. SmartGridComm*, Oct. 2010, pp. 244–249.
[12] N. Hadjsaid, C. Tranchita, B. Rozel, M. Viziteu, and R. Caire, "Modeling cyber and physical interdependencies—Application in ICT and power grids," in *Proc. IEEE/PES Power Syst. Conf. Expo.*, Mar. 2009, pp. 1–6.
[13] G. Dondossola, F. Garrone, and J. Szanto, "Cyber risk assessment of power control systems—A metrics weighed by attack experiments," in *Proc. IEEE Power Energy Soc. Gen. Meet.*, 2011, pp. 1–9.
[14] J.-C. Laprie, K. Kanoun, and M. Kaaniche, "Modelling interdependencies between the electricity and information infrastructures," in *Proc. Int. Conf. Comput. Saf. Reliab. Security*, 2007, pp. 54–67.
[15] S. Delamare, A.-A. Diallo, and C. Chaudet, "High-level modelling of critical infrastructures' interdependencies," *Int. J. Crit. Infrastruct.*, vol. 5, no. 1, pp. 100–119, 2009.
[16] J. Sanchez, R. Caire, and N. Hadjsaid, "ICT and power distribution modeling using complex networks," in *Proc. IEEE PowerTech*, 2013, pp. 1–6.
[17] D. Bienstock, "Optimal control of cascading power grid failures," in *Proc. IEEE Decision Control/Eur. Control Conf.*, 2011, pp. 2166–2173.
[18] R. Majumder, B. Chaudhuri, B. C. Pal, and Q.-C. Zhong, "A unified Smith predictor approach for power system damping control design using remote signals," *IEEE Trans. Control Syst. Technol.*, vol. 13, no. 6, pp. 1063–1068, Nov. 2005.
[19] K. Natori and K. Ohnishi, "A design method of communication disturbance observer for time-delay compensation, taking the dynamic property of network disturbance into account," *IEEE Trans. Ind. Electron.*, vol. 55, no. 5, pp. 2152–2168, May 2008.
[20] D. Zhi, L. Xu, and B. W. Williams, "Model-based predictive direct power control of doubly fed induction generators," *IEEE Trans. Power Electron.*, vol. 25, no. 2, pp. 341–351, Feb. 2010.
[21] P. Cortes, J. Rodriguez, C. Silva, and A. Flores, "Delay compensation in model predictive current control of a three-phase inverter," *IEEE Trans. Ind. Electron.*, vol. 59, no. 2, pp. 1323–1325, Feb. 2012.
[22] J. Rodriguez *et al.*, "State of the art of finite control set model predictive control in power electronics," *IEEE Trans. Ind. Informat.*, vol. 9, no. 2, pp. 1003–1016, May 2013.
[23] A. N. Venkat, I. A. Hiskens, J. B. Rawlings, and S. J. Wright, "Distributed MPC strategies with application to power system automatic generation control," *IEEE Trans. Control Syst. Technol.*, vol. 16, no. 6, pp. 1192–1206, Nov. 2008.
[24] T. Mohamed, H. Bevrani, A. Hassan, and T. Hiyama, "Decentralized model predictive based load frequency control in an interconnected power system," *Energy Convers. Manage.*, vol. 52, no. 2, pp. 1208–1214, Feb. 2011.
[25] R. Yang, G. Liu, P. Shi, C. Thomas, and M. Basin, "Predictive output feedback control for networked control systems," *IEEE Trans. Ind. Electron.*, vol. 61, no. 1, pp. 512–520, Jan. 2014.
[26] J. Fischer, S. Gonzalez, M. Herran, M. Judewicz, and D. Carrica, "Calculation-delay tolerant predictive current controller for three-phase inverters," *IEEE Trans. Ind. Informat.*, vol. 10, no. 1, pp. 233–242, Feb. 2014.
[27] C. Xia, T. Liu, T. Shi, and Z. Song, "A simplified finite control set model predictive control for power converters," *IEEE Trans. Ind. Informat.*, vol. 10, no. 2, pp. 991–1001, May 2014.
[28] Y. Zhang, W. Xie, Z. Li, and Y. Zhang, "Low complexity model predictive power control: Double-vector-based approach," *IEEE Trans. Ind. Electron.*, vol. 61, no. 11, pp. 5871–5880, Nov. 2014.
[29] D. Bienstock and A. Verma, "The N-k problem in power grids: New models, formulations, numerical experiments," *SIAM J. Optim.*, vol. 20, no. 5, pp. 2352–2380, Apr. 2010.
[30] D. Bienstock, M. Chertkov, and S. Harnett, "Chance constrained optimal power flow: Risk-aware network control under uncertainty," *arXiv preprint*, vol. arXiv:1209.5779, 2012.

[31] A. Bernstein, D. Bienstock, D. Hay, M. Uzunoglu, and G. Zussman, "Power grid vulnerability to geographically correlated failures—Analysis and control implications," *arXiv preprint*, vol. arXiv:1206.1099, 2012.
[32] E. F. Camacho and C. B. Alba, *Model Predictive Control*. Berlin, Germany: Springer-Verlag, 2013.
[33] S. J. Qin and T. A. Badgwell, "A survey of industrial model predictive control technology," *Control Eng. Pract.*, vol. 11, no. 7, pp. 733–764, Jul. 2003.

Luca Galbusera received the M.Sc. degree in systems and control engineering and the Ph.D. degree in information engineering from the Politecnico di Milano, Milan, Italy, in 2006 and 2010, respectively.

He has held postdoctoral research positions with the Politecnico di Milano and with the Institute of Applied Mathematics and Information Technology, Italian National Research Council (CNR-IMATI). He is currently a Scientific Officer with the Institute for the Protection and Security of the Citizen, European Commission Joint Research Centre, Ispra, Italy. His research interests include switched systems, optimal and robust control, model predictive control, multiagent systems, networked control systems, and resilience in critical infrastructures.

Dr. Galbusera was a recipient of the "Giorgio Quazza" Prize from the Politecnico di Milano in 2006.

Georgios Theodoridis received the M.Sc. and Ph.D. degrees in electrical and computer engineering, with an expertise in telecommunications, from Aristotle University of Thessaloniki, Thessaloniki, Greece, in 2004 and 2010, respectively.

He has been involved in numerous European and national research projects with the Institute for the Protection and Security of the Citizen, European Commission Joint Research Centre, Ispra, Italy. His research interests are in resource management and quality of service guarantees for wireless/mobile telecommunications systems, as well as in the area of network security, regarding the detection, identification, root cause attribution, and mitigation of anomalies in telecommunication networks, with a special focus on critical infrastructures.

Georgios Giannopoulos received the M.Sc. degree in mechanical and aeronautical engineering from the University of Patras, Greece, in 1999, the M.Sc. degree in management from Solvay Brussels School of Economics and Management, Belgium, in 2005, and the Ph.D. degree in engineering from Vrije Universiteit Brussel, Belgium, in 2007.

Since 2007, he has been a Scientific Officer with the Institute for the Protection and Security of the Citizen of the European Commission's Joint Research Centre, Ispra, Italy. He is currently working in the domain of critical infrastructures risk and resilience modeling with focus on systems of systems perspective. In this framework, he is carrying out research in the domain of GIS for risk assessment and resilience for critical infrastructures, interdependencies between ICT and power systems, and economic impact of critical infrastructure disruption.